Unveiling the engine of the Sun: Measurements of the *pp*-chain solar neutrinos with Borexino

D. Guffanti[1,†], A.C. Re[2], O. Smirnov[3]

[1] *Institute of Physics and Excellence Cluster PRISMA+, Johannes Gutenberg-Universität Mainz, 55099, Mainz, Germany*
daniele.guffanti@uni-mainz.de

[2] *Dipartimento di Fisica "A. Pontremoli", Università degli Studi and INFN Milano, 20133 Milano, Italy*
alessandra.re@mi.infn.it

[3] *Joint Institute for Nuclear Research, 141980 Dubna, Russia*
oleg.smirnov@lngs.infn.it

on behalf of the Borexino Collaboration:
M. Agostini, K. Altenmüller, S. Appel, V. Atroshchenko, Z. Bagdasarian, D. Basilico, G. Bellini, J. Benziger, R. Biondi, D. Bravo, B. Caccianiga, F. Calaprice, A. Caminata, P. Cavalcante, A. Chepurnov, D. D'Angelo, S. Davini, A. Derbin, A. Di Giacinto, V. Di Marcello, X.F. Ding, A. Di Ludovico, L. Di Noto, I. Drachnev, A. Formozov, D. Franco, C. Galbiati, C. Ghiano, M. Giammarchi, A. Goretti, A.S. Göttel, M. Gromov, Aldo Ianni, Andrea Ianni, A. Jany, D. Jeschke, V. Kobychev, G. Korga, S. Kumaran, M. Laubenstein, E. Litvinovich, P. Lombardi, I. Lomskaya, L. Ludhova, G. Lukyanchenko, L. Lukyanchenko, I. Machulin, J. Martyn, E. Meroni, M. Meyer, L. Miramonti, M. Misiaszek, V. Muratova, B. Neumair, M. Nieslony, R. Nugmanov, L. Oberauer, V. Orekhov, F. Ortica, M. Pallavicini, L. Papp, L. Pelicci, Ö. Penek, L. Pietrofaccia, N. Pilipenko, A. Pocar, G. Raikov, M.T. Ranalli, G. Ranucci, A. Razeto, M. Redchuk, A. Romani, N. Rossi, S. Schönert, D. Semenov, G. Settanta, M. Skorokhvatov, A. Singhal, A. Sotnikov, Y. Suvorov, R. Tartaglia, G. Testera, J. Thurn, E. Unzhakov, F. Villante, A. Vishneva, R.B. Vogelaar, F. von Feilitzsch, M. Wojcik, M. Wurm, S. Zavatarelli, K. Zuber, and G. Zuzel.

About 99% of solar energy is produced through sequences of nuclear processes that convert Hydrogen into Helium in the so-called *pp*-chain. The neutrinos emitted in five of these reactions represent a unique probe of the Sun's internal working and, at the same time, offer an intense natural neutrino beam for fundamental physics research.

The Borexino experiment consists of a large-volume liquid-scintillator detector designed and constructed for real-time detection of low energy solar neutrinos. It is installed at the underground INFN Laboratori Nazionali del Gran Sasso (L'Aquila, Italy) and started taking data in May 2007. Borexino has been the only experiment so far capable of performing a complete study of the *pp*-chain by directly measuring the neutrino-electron

[†] Current address: Dipartimento di Fisica "G. Occhialini", Università degli Studi and INFN Milano Bicocca, 20126 Milano, Italy.

elastic scattering rates for the neutrinos produced in four of its reactions: the initial proton–proton (*pp*) fusion, the electron capture of Beryllium-7, the proton–electron–proton (*pep*) fusion, and the Boron-8 β^+ decay. A limit on the neutrino flux produced in the helium-proton fusion (hep) was also set. This set of measurements further probes the solar fusion mechanism via the direct determination of the relative intensity of the two primary terminations of the *pp*-chain, and the computation of the solar neutrino luminosity. Moreover, the Beryllium-7 and Boron-8 fluxes are indicative of the Sun's core temperature, and their measurement shows a mild preference for the higher temperature expected from the high-metallicity Standard Solar Model scenario. Finally, the experimental survival probability of these solar electron neutrinos allows to simultaneously probe the MSW neutrino flavor conversion paradigm, both in vacuum and in matter-dominated regimes, at different energies.

The details of the strategy adopted by the Borexino collaboration for successfully isolating the spectral components of the *pp*-chain neutrinos signal from residual backgrounds in the total energy spectrum will be presented.

Keywords: Solar neutrinos, proton-proton chain, Borexino

1. Introduction

The study of neutrinos generated by nuclear processes in the Sun has been producing outstanding scientific results for more than 50 years in both the fields of astrophysics and particle physics. The measurements of solar neutrinos provided the first direct evidence of the nuclear origin of stars' luminosity, as well as the first indication of flavour transition in the neutrino sector. In the years, solar neutrino experiments have progressively improved their accuracy, bringing new insights on the functioning of the Sun and on the properties of neutrinos.

The Borexino experiment is a key player in this field, being the most sensitive detector so-far for low-energy solar neutrinos. One of the milestones of the Borexino physics program, which significantly exceeded the expected physics reach, is the (almost) complete investigation of neutrinos produced throughout the entire proton-proton fusion chain, the sequence of nuclear reactions responsible for $\approx 99\%$ of the Sun luminosity. This fundamental result, partially achieved already during the first phase of the experiment (2007-2010), has been further improved in the phase II (2011-2016) and made it possible to test our knowledge of the Sun and to constrain exotic properties of neutrinos.

We present in this contribution the latest results of Borexino regarding solar neutrinos emitted throughout the *pp*-chain and we discuss their implications for both neutrino and solar physics. Section 2 describes the proton-proton fusion chain and the neutrinos produced therein, while the Borexino detector is presented in Sec. 3. The spectrum of solar neutrinos spans across a wide energy range extended up to 19 MeV and their fluxes vary of several orders of magnitude, therefore we setup two separate analyses targeting the low- and high-energy region of the solar neutrino spectrum that are described in Secs. 4 and 5 respectively along with the main results of Borexino.

2. Solar neutrinos from the *pp*-chain

The Sun, as most of other stars, produces energy by fusing four protons into a helium nucleus. This idea, originally hypothesized by Perrin and Eddington,[1,2] was later formalized by Bethe and Critchfield and independently by Weizsäcker who proposed two mechanisms for the hydrogen burning, known as the proton-proton chain[3] (*pp*-chain) and the Carbon-Nitrogen-Oxygen (CNO) cycle.[4–6] The relative efficiency of these two processes depends heavily on the features of the star under consideration, specifically on its core temperature and on its chemical composition. While the CNO-cycle was initially believed to be the dominant energy-production mechanism in the Sun, in light of a more accurate estimate of the Sun core temperature it became clear that the *pp*-chain drives the energy production in the Sun. The relative weight of the two mechanisms is estimated by a detailed model of the Sun, also known as Standard Solar Model (SSM), which -provided an accurate description of all the physical processes driving the evolution of a star- is able to produce a comprehensive snapshop of the Sun by forcing the modelled star to match the current solar mass, radius, luminosity and surface composition. The most recent update of the SSM[7] indicates that only $\approx 1\%$ of the Sun energy is produced through the CNO-cycle, while the real "engine" of the Sun is the *pp*-chain, accounting for $\approx 99\%$ of the Sun luminosity.

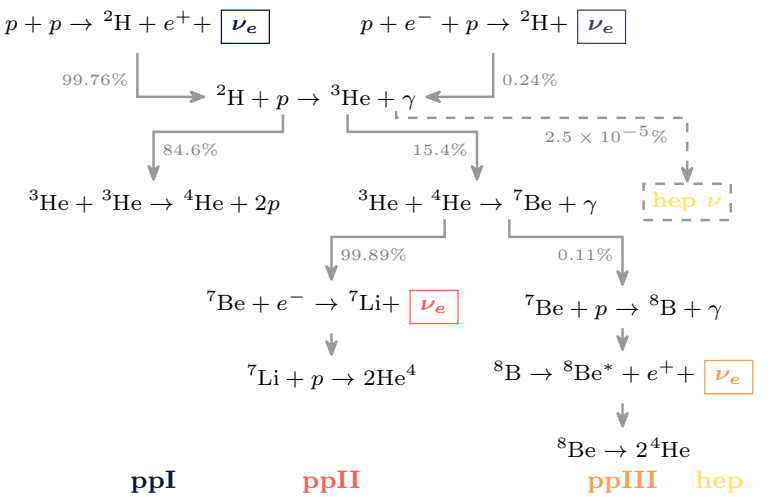

Fig. 1. The sequence of reactions composing the proton-proton fusion chain.

The sequence of reactions composing the *pp*-chain is shown in Fig. 1. Neutrinos are emitted in five of such processes, starting with the fusion of two protons into a deuteron which begins the chain (*pp* neutrinos). An alternative way of producing a deuteron, although $\approx$ 400 times less likely than the proton-proton fusion,

consists in the reaction between two protons and an electron, which releases a 1.44 MeV monoenergetic neutrino (*pep* neutrino). The *pp*-chain can progress into different branches, namely ppI, ppII, ppIII and hep. Depending on the evolution of the chain, different neutrinos can be emitted: while the most prominent branch (ppI) terminates the chain without releasing any additional neutrino, the ppII branch is characterized by monoenergetic neutrinos produced by electron-capture onto ^{7}Be, with energy of 0.86 MeV (branching ratio 89.5%) or 0.38 MeV (B.R. 10.5%) depending if the ^{7}Li nucleus in the final state is produced at its ground state or on the first excited state. The high-energy neutrinos emitted in the decay of ^{8}B (Q-value 15.5 MeV) tag the ppIII branch, and the faintest branch of all, the helium-proton fusion (hep) branch, produces neutrinos up to an energy of 19.8 MeV. The expected solar neutrino spectrum is shown in Fig. 2.

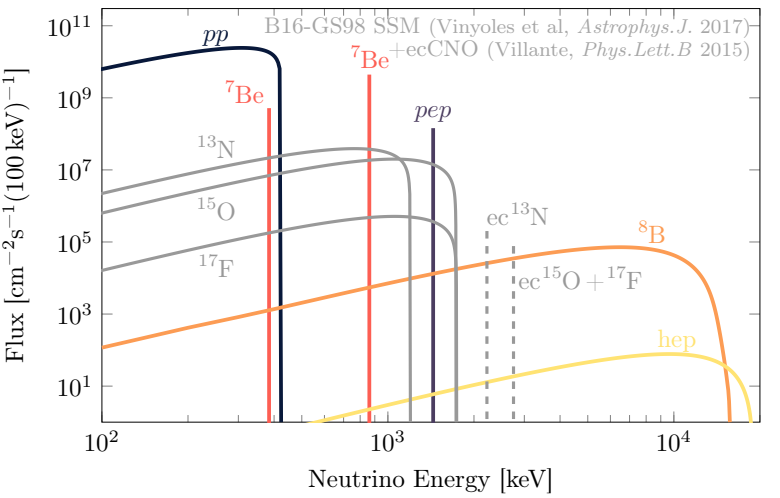

Fig. 2. Expected solar neutrino spectrum, with the neutrinos originating from the *pp*-chain shown with coloured lines and those produced in the CNO-cycle in grey. The fluxes are taken from[7,8] (note that the flux of monoenergetic neutrinos is reported in $\mathrm{cm}^{-2}\,\mathrm{s}^{-1}$).

The fluxes of *pp*-chain solar neutrinos depends on the abundance of heavy elements in the Sun, which is currently not fully understood and affects the temperature profile thus impacting on the *pp*-chain nuclear reactions rate. Recent estimates of the photosphere composition[9] (AGSS09met) show a consistent reduction of the metallicity respect to previous studies[10] (GS98), but this new "low-metallicity" (LZ) SSM shows a worst agreement with observation of the sound speed profile as inferred by helioseismology measurements respect to the old "high-metallicity" (HZ) predictions.[7] The precision measurement of solar neutrino fluxes from the *pp*-chain and the CNO-cycle is a promising way to solve the controversy about solar metallicity and the impact of Borexino results in this connection is discussed in Sec. 6.

3. The Borexino experiment

The Borexino experiment can detect solar neutrinos which interact via elastic scattering with the electrons of a liquid scintillator (LS). This detection technique, which provides a low-energy threshold and a good energy resolution, makes it possible to separate the different components of the solar neutrino flux exploiting their specific signature in the energy spectrum, but requires an extremely careful strategy to reduce the indistinguishable radioactive background since the expected interaction rate is ≈ 9 orders of magnitude smaller than the average activity of ordinary water.

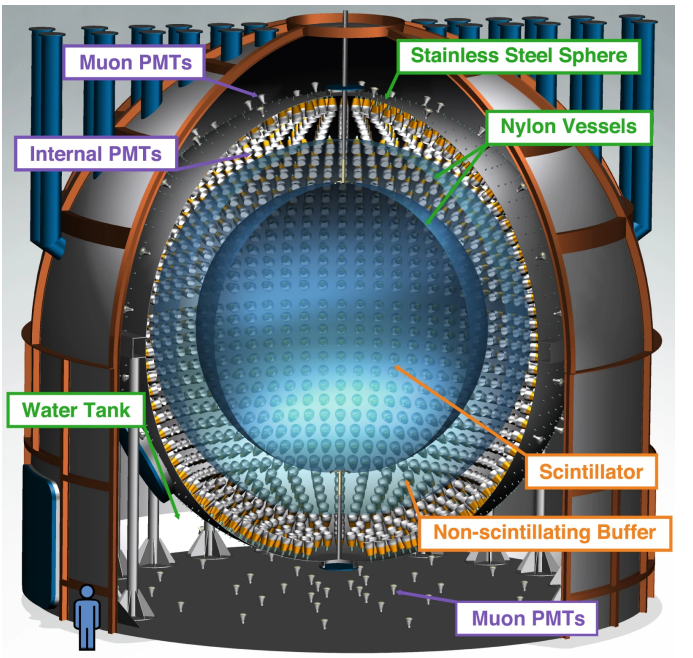

Fig. 3. Schematic view of the Borexino detector. Figure from.[11]

A cutaway of the detector is shown in Fig. 3. The experiment[12] is located in the INFN Gran Sasso National Laboratories, under the Gran Sasso massif in L'Aquila (Italy). The underground laboratories are shielded from cosmic radiation by 1400 m or rock (3800 m.w.e.), which attenuates the cosmic-ray flux by 6 orders of magnitude. Residual muons still reaching the experimental hall[13] ($3.432 \pm 0.003\,\mathrm{cm}^{-2}\,\mathrm{s}^{-1}$) are tagged using a water Cherenkov detector equipped with 208 PMTs which surrounds the entire inner detector also providing an effective shielding against environmental neutrons and γ-rays. The detector active volume consists of ≈ 300 ton of pseudocumene mixed with 1.5 g/l of (PPO) as a wavelength shifter and is contained into a 125 µm-thick, 4.25 m radius spherical nylon vessel (Inner Vessel, IV). The light

produced by the energy deposition of charged particles is detected by 2212 8 in PMTs (1800 of which are equipped with a light collector cone) mounted onto a 6.85 m radius Stainless Steel Sphere. The space between the IV and the PMTs is filled with quenched LS in order to shield the active volume from the radiation coming from radioactive contamination in the PMTs' glass and in the steel of the support structure.

With the underground location and shielding strategies fighting the external background, the key of Borexino results has been the successful suppression of internal background, *i.e.* those radioactive contamination of the detector itself. This has been achieved thanks to a careful selection of materials and to the implementation of effective purification methods for the LS (primarily distillation and water extraction) which reduced the contamination of ^{238}U and ^{232}Th down to $< 9.5 \times 10^{-20}$ g/g and $< 7.2 \times 10^{-19}$ g/g respectively in the Phase II of the experiment.[14]

The reconstruction of the solar neutrino interaction rate and its separation from the residual background is based primarily (although not exclusively) on the signatures in the visible energy spectrum reconstructed from the scintillation light, therefore the understanding of the detector energy response is fundamental. The energy released in the detector is reconstructed by measuring the isotropic scintillation light produced by recoiling electrons in the LS; the information about the detected light is expressed using three different energy observable that are used in the analysis: the number of hit PMTs in a 230(400) time window ($N_p^{dt_{1(2)}}$), the number of reconstructed hits (N_h) and the total charge measured at the PMTs anode, *i.e.* the number of detected photoelectrons (N_{pe}).

Borexino can rely on two different methods to model the detector response function: the first is based on a full Monte Carlo (MC) simulation of the entire experimental apparatus,[15] which reproduces all the physical processes following the interaction of a particle in the detector (including the electronic chain response) and keeps track of evolution of the detector properties in time, such as the number of operating channels. The simulation has been tuned using both lab measurements and data collected in an extensive calibration campaign,[16] resulting in a sub-percent accuracy for the variables of interest for solar neutrino analysis.[15] An alternative method for modelling the detector energy response consists in an analytical model encapsulating the effect of ionization quenching, the contribution of Cherenkov light as well as the spatial dependence of the reconstructed energy and of the energy resolution.[14] With such model it is possible to reproduce the observed energy spectrum of a given signal by computing the convolution of the visible energy spectrum with the detector response function. More details about this procedure can be found in.[14]

The performance of the detector and the reliability of the response models have been carefully studied during the calibration campaign[16] and are constantly monitored using some known background (such as the ^{14}C, cosmogenic ^{11}C or the characteristic peak of ^{210}Po, see Sec. 4). During the Phase II of Borexino data taking, the energy resolution for 1 MeV deposited energy was close to 50 keV, while the

position of the event –reconstructed via a time-of-flight method– had an accuracy of $\approx 10\,\mathrm{cm}$

4. Low-Energy solar neutrino spectroscopy

The observation of low-energy solar neutrinos has been one of the main goal of the experiment, given their fundamental importance for both neutrino- and solar physics. Differently from the previous generation of low-energy solar neutrino experiments, which were able to measure the integrated neutrino flux over a given energy threshold, the key advantage of Borexino is the possibility to separate the individual contribution of neutrinos produced in different reactions thanks to their specific signature in the visible energy spectrum.

Already during the first phase[17] of the experiment Borexino was able to measure the interaction rate of ^{7}Be, ^{8}B and *pep* neutrinos,[18–20] while imposing an upper limit to the rate of CNO neutrinos.[20] We present in this section the result obtained from the analysis of low-energy neutrinos obtained in the second phase of the Borexino data taking, started in 2011 following a very successful purification campaign which further reduced the already low contamination level in the liquid scintillator. In Sec. 4.1 we discuss the measurement of *pp*-chain low-energy neutrinos reported in,[11,14] while in 4.2 we show the evidence of the time modulation of solar neutrinos interaction rate expected from the Earth's orbit eccentricity. In the second part of this section we report the search of exotic properties of neutrinos performed using low-energy solar neutrinos: in particular Sec. 4.3 presents a limit on the neutrino magnetic moment, while we discuss in Sec. 4.4 the search for neutrino non-standard interactions.

Given their low-flux and different energy scale, neutrinos from the ^{8}B decay require a separate analysis, which is presented in Sec. 5.

4.1. *Simultaneous measurement of low-energy solar neutrino fluxes*

The latest measurements of low-energy solar neutrinos produced by the *pp*-chain performed by Borexino is based on a dataset collected between December 14^{th}, 2011 and May 21^{st}, 2016 (1291.51 days). The increased exposure ($\approx$ 1.6 times larger than Phase I), combined with the lower contamination background and the improved understanding of the detector made it possible to simultaneously extract all the interaction rates of the low-energy components of the *pp*-chain in a single fit over a large portion of the energy spectrum (0.19–2.93 MeV), differently from previous Borexino results where the different solar neutrino species were studied separately optimising the choice of the energy window.

Data recorded by the detector are filtered to remove residual cosmic muons and short-living cosmogenic isotopes by applying a 300 ms veto.[14] In order to remove "external" γ-ray background generated in the material surrounding the liquid

scintillator (especially in the PMTs and in the nylon of the inner vessel) we select only those events reconstructed in a 71.3 tonnes fiducial volume defined in the innermost part of the detector.[14]

The reconstruction of solar neutrinos interaction rates from the energy spectrum is made more challenging by the presence of multiple backgrounds that still contaminates the dataset even after the successful purification of the scintillator and the data selection outlined above: in particular, the sensitivity of Borexino in the low-energy part of the spectrum is limited by the presence of ^{14}C in the LS molecules (β^-, $Q = 0.16\,\mathrm{MeV}$), which decay in the detector at an much higher rate than solar neutrino interactions. Other contamination affecting the energy window are ^{85}Kr (β^-, $Q = 0.69\,\mathrm{MeV}$), ^{210}Po (α, $E_\alpha = 5.3\,\mathrm{MeV}$, light quenched by a factor ≈ 10 in LS) and ^{210}Bi (β^-, $Q = 1.16\,\mathrm{MeV}$). At higher energies, the relevant background is mostly due to residual "external" γ-rays and to cosmogenic ^{11}C (β^+, $Q = 0.96\,\mathrm{MeV}$). The latter can be efficiently tagged by exploiting the fact that it is often produced together with one or more neutrons following muon spallation onto ^{12}C, therefore one can evaluate the likelihood for an event to be a ^{11}C decay on the basis of a set of observables such as the distance and time interval from a crossing muon, the distance of a detected neutron capture and the muon energy deposition profile.[21] Using this selection it has been possible to tag $(92 \pm 4)\,\%$ of ^{11}C events retaining $(64.28 \pm 0.01)\,\%$ of the total exposure, and those events classified as likely to be ^{11}C decays are used to build a separate, ^{11}C-tagged dataset that is analysed jointly with ^{11}C suppressed one.

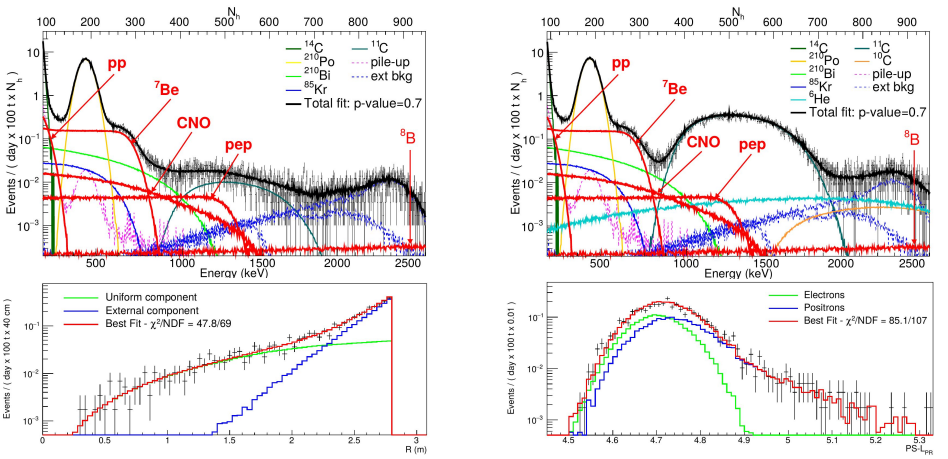

Fig. 4. Result of the simultaneous measurement of low-energy *pp*-chain solar neutrinos. *Top panel*: visible energy spectra in the ^{11}C-subtracted (left) and -tagged datasets. *Bottom left*: Distribution of the events distance from the detector centre. *Bottom right*: Distribution of the pulse shape parameter. All figures from.[14]

To help constraining some of these backgrounds, in some specific cases it is possible to rely on some distinctive features of the signal or on some independent measurements: this is the case of the rate of ^{14}C, which has been measured using a separate dataset to be 40 ± 1 Bq/100 t and that was constrained in the analysis together with the rate of random coincidences of ^{14}C decays. Differently, the signal from external γ-rays shows a clear exponential decrease towards the detector centre due to the shielding effect of LS, while energy release of positrons emitted in the β^+ decay of ^{11}C and its subsequent annihilation results in a slightly different time profile, that we used to define a Pulse Shape (PS) parameter[14] that improves the separation between β^+ and β^-events. In order to take into account these features, we implemented a multivariate analysis which include the events' distance from the detector centre and pulse shape parameter in addition to the energy observables in the region where they can help the analysis.

The analysis procedure has been tested running a detailed sensitivity study[14] based on simulated experiments. This study showed a significant correlation between the reconstructed rates of *pep*, CNO end ^{210}Bi events, which led to a reduced sensitivity for such parameters. For this reason, we decided to constrain in the analysis the rate of CNO neutrinos to the value expected from the prediction of the SSM (both HZ and LZ). The results of the fit[11,14] are reported in Tab. 1 next to the expectations from the SSM,[7] assuming the MSW-LMA oscillation parameters.[22] Similarly, the lower part of Tab. 1 reports the fluxes of solar netrinos inferred from Borexino measurements assuming the MSW-LMA solution. Figure 4 shows the different contributions of solar neutrinos and backgrounds to the energy spectrum as well as to the radial distance and pulse shape distributions.

Systematic uncertainties in the measurement account for possible deviations of the computed exposure, uncertainties in the detector response model as well as specific effects of the analysis methods.[11,14]

The results in Tab. 1 represents the most accurate experimental measurements of low-energy solar neutrinos from the *pp*-chain, improving Borexino previous findings: in particular, the interaction rate of ^{7}Be neutrinos is constrained at the 3 % level, twice as accurate as the expectation of the SSM, while the absence of *pep* neutrinos is disfavoured with a 5σ significance.

4.2. *Time modulations of neutrino signal*

The solar neutrino signal should follow the annual variations of the Sun-to-Earth distance, the effect appears as a 6.7% peak-to-peak seasonal amplitude modulation, with a maximum at the perihelion. The observation of seasonal variation would confirm the solar origin of the signal. Another possible modulation could be induced due to the Earth matter: neutrino are passing through the dense matter in the night and this could cause flavour regeneration with probability dependent on

Table 1. Results of Borexino-Phase II on the *pp*, ^{7}Be and *pep* solar neutrinos interaction rate. The first term of the associated uncertainty represents the statistical error obtained with a likelihood profile under the Wilk's approximation, while the second indicates the systematic uncertainty. The *pep* neutrino rate depends on the different SSM used to constrain the CNO neutrino flux, and therefore two results are quoted. The fluxes reported in the lower part of the table are computed assuming the MSW-LMA oscillation parameters[22]

Solar ν	**Borexino results** Rate (cpd/100 t)	**HZ SSM** Rate (cpd/100 t)	**LZ SSM** Rate (cpd/100 t)
pp	$134 \pm 10^{+6}_{-10}$	131.0 ± 2.4	132.1 ± 2.3
^{7}Be	$48.3 \pm 1.1^{+0.4}_{-0.7}$	47.8 ± 2.9	43.7 ± 2.6
pep (HZ)	$2.43 \pm 0.36^{+0.15}_{-0.22}$	2.74 ± 0.05	2.78 ± 0.05
pep (LZ)	$2.65 \pm 0.36^{+0.15}_{-0.24}$		
	Flux cm^{-2}s^{-1}	Flux cm^{-2}s^{-1}	Flux cm^{-2}s^{-1}
pp	$(6.1 \pm 0.5^{+0.3}_{-0.5}) \times 10^{10}$	$5.98(1 \pm 0.006) \times 10^{10}$	$6.03(1 \pm 0.005) \times 10^{10}$
^{7}Be	$(4.99 \pm 0.13^{+0.07}_{-0.10}) \times 10^9$	$4.93(1 \pm 0.06) \times 10^9$	$4.50(1 \pm 0.06) \times 10^9$
pep (HZ)	$(1.27 \pm 0.19^{+0.08}_{-0.12}) \times 10^8$	$1.44(1 \pm 0.009) \times 10^8$	$1.46(1 \pm 0.009) \times 10^8$
pep (LZ)	$(1.39 \pm 0.19^{+0.08}_{-0.13}) \times 10^8$		

the oscillation parameters. The fact of observation or non-observation of diurnal modulation can be used to restrict the neutrino oscillation parameters.

The seasonal modulation of the ^{7}Be neutrino signal was studied by Borexino collaboration in,[17,23] The earlier work was performed with Borexino Phase-I data acquired from May 2007 to May 2010; the period and phase were found to be consistent with a solar origin of the signal. More advanced analysis of 1456 astronomical days of Phase-II data can be found in more recent paper.[23] The analysis of neutrino signal variations on the many years time-scale is complicated by the presence of time-dependent background components. Three methods have been used to extract the time modulations: the analytical fit to event rate, and two more elaborated techniques: Lomb-Scargle and the Empirical Mode Decomposition. The results obtained with these methods are in excellent agreement. The duration of astronomical year measured with neutrino by using fit to the event rate is 367 ± 10 days with phase shift of $T_0 = 14 \pm 22$ days, i.e. in good agreement with the expected values. Also, the observe eccentricity $\epsilon = 0.0174 \pm 0.0045$ corresponds to the modulation amplitude of $(7.1 \pm 1.9)\%$.

In contrast to the annual signal modulation, no variation of day/night solar neutrino signal at the level of 1% is observed in Borexino data.[24] The measured asymmetry $A_{dn} = 0.001 \pm 0.012(stat) \pm 0.007(syst)$ agrees with the prediction of LMA solution for MSW mechanism. Moreover, this result disfavours MSW oscillations with mixing parameters in the LOW region at more than 8.5σ. The LOW

solution was previously excluded by using the reactor antineutrino data, which involves the assumption of CPT symmetry.

4.3. *Neutrino magnetic moment*

One of the explanation of recent puzzling result of the XENON1T collaboration at few keV electronic recoils could be due to the scattering of solar neutrinos with large Majorana transition magnetic moments[25] (MM). The required transition MM strengths lie within the range that can be probed by current or near future experiments.

Borexino is spectroscopic detector with a relatively good energy resolution at low energies of about 5% at 1 MeV. The spectroscopic feature provides a good possibility to search for the deviations from the standard shape of recoils electrons scattered off monoenergetic ^{7}Be neutrinos. The manifestation of the large neutrino magnetic moment in the electron recoils spectrum would be an additional term in the cross section with a characteristic $1/\mathrm{T}_e$ (T is electron recoil kinetic energy) signature. A sensitive search for the deviations of the electron recoil spectra from the predicted by the Standard Model was performed using Borexino Phase-II data in.[26] A model-independent limit on the effective moment of the solar neutrino of $\mu_{\text{eff}} < 2.810^{-11}\,\mu_B$ at 90% C.L. was obtained. This could be compared to the best direct limit on the magnetic moment of electron antineutrino $\mu_{\text{eff}} < 2.910^{-11}\,\mu_B$ at 90% C.L. obtained using Ge detectors in the most sensitive reactor experiment GEMMA.[27] The Borexino limit is free from uncertainties associated with predictions of the SSM neutrino flux and with the detector's fiducial volume, and is obtained by constraining the sum of the solar neutrino fluxes using the results from radiochemical (gallium) experiments.

Since neutrinos are a mixture of mass eigenstates the effective magnetic moment for neutrino-electron scattering is:

$$\mu^2_{\text{eff}} = \sum_j |\sum_k \mu_{kj} A_k(E_\nu, L)|^2, \tag{1}$$

where μ_{jk} is an element of the neutrino electromagnetic moments matrix and $A_k(E_\nu, L)$ is the amplitude of the k-mass state at the point of scattering. For the Majorana neutrino, only the transition moments are nonzero, while the diagonal elements of the matrix are equal to zero due to CPT-conservation. For the Dirac neutrino, all matrix elements may have nonzero values. The effective magnetic moment can be expanded both in terms of the mass eigenstates or the flavor eigenstates.

In the general case the expression for the effective magnetic moment in the mass eigenstate basis will have a complex form consisting of interference terms $\propto \mu_{jk}\mu_{ik}$. Without significant omissions the solar neutrinos arriving at the Earth can be considered as an incoherent mixture of mass eigenstates. In the case of Dirac

neutrinos assuming that only diagonal magnetic moments μ_{ii} are nonvanishing:

$$\mu^2_{\text{eff}} = P^{3\nu}_{e1}\mu^2_{11} + P^{3\nu}_{e2}\mu^2_{22} + P^{3\nu}_{e3}\mu^2_{33} \tag{2}$$

where $P^{3\nu}_{ei} = |A_i(E,L)|^2$ is the probability of observing the i-mass state at the scattering point for an initial electron flavor.

In the case of Majorana transition magnetic moments the effective moment is:

$$\mu^2_{\text{eff}} = P^{3\nu}_{e1}(\mu^2_{12} + \mu^2_{13}) + P^{3\nu}_{e2}(\mu^2_{21} + \mu^2_{23}) + P^{3\nu}_{e3}(\mu^2_{31} + \mu^2_{32}) \tag{3}$$

For the well-known approximation of three- to two- neutrino oscillation probabilities for solar neutrinos: $P^{3\nu}_{e1} = \cos^2\theta_{13}P^{2\nu}_{e1}$, $P^{3\nu}_{e2} = \cos^2\theta_{13}P^{2\nu}_{e2}$ and $P^{3\nu}_{e3} = \sin^2\theta_{13}$ – one can get the effective magnetic moment expressed in well-established oscillation parameters in the mass eigenstate basis. Equation (2) can be rewritten as:

$$\mu^2_{\text{eff}} = C^2_{13}P^{2\nu}_{e1}\mu^2_{11} + C^2_{13}P^{2\nu}_{e2}\mu^2_{22} + S^2_{13}\mu^2_{33} \tag{4}$$

where $C^2_{13} \equiv \cos^2\theta_{13}$ and $S^2_{13} \equiv \sin^2\theta_{13}$, and $P^{2\nu}_{e1} + P^{2\nu}_{e2} = 1$. Similarly, assuming CPT-conservation ($\mu_{jk} = \mu_{kj}$) relation (3) for the transition moments can be rewritten as:

$$\mu^2_{\text{eff}} = C^2_{13}P^{2\nu}_{e1}\mu^2_{12} + (1 - C^2_{13}P^{2\nu}_{e2})\mu^2_{13} + (1 - C^2_{13}P^{2\nu}_{e1})\mu^2_{23} \tag{5}$$

In general, $P^{2\nu}_{e1}$ and $P^{2\nu}_{e2}$ (and $P^{2\nu}_{ee}$) depend on the neutrino energy, but in the energy region below 1 MeV the probabilities can be assumed constant.

Since μ^2_{eff} is the sum of positively defined quantities, one can constrain any term in (4) and (5). By using the most probable values of $P^{2\nu}_{ee}$, θ_{12} and θ_{13} one can obtain the following limits from the relation $\mu_{\text{eff}} \leq 2.8 \times 10^{-11}\mu_B$:

$$|\mu_{11}| \leq 3.4; \quad |\mu_{22}| \leq 5.1; \quad |\mu_{33}| \leq 18.7; \tag{6}$$

$$|\mu_{12}| \leq 2.8; \quad |\mu_{13}| \leq 3.4; \quad |\mu_{23}| \leq 5.0; \tag{7}$$

all measured in units of $10^{-11}\mu_B$ and for 90% C.L.

The effective magnetic moment for the LMA-MSW solution in flavour basis assuming the survival probability of *pp* and ^{7}Be solar neutrinos is the same:

$$\mu^2_{\text{eff}} = P^{3\nu}\mu^2_e + (1 - P^{3\nu})(\cos^2\theta_{23} \cdot \mu^2_\mu + \sin^2\theta_{23} \cdot \mu^2_\tau), \tag{8}$$

where $P^{3\nu} = \sin^4\theta_{13} + \cos^4\theta_{13}P^{2\nu}$ is the probability that ν_e is detected in its original flavor (survival probability), with $P^{2\nu}$ calculated in the "standard" 2-neutrino scheme, θ_{13} and θ_{23} are the corresponding mixing angles. Though $P^{2\nu}$ depends on E_ν, the difference between $P^{2\nu}(400) = 0.57$ for a neutrino energy close to the *pp*-neutrino spectrum end point of 420 keV (only a small fraction of the total *pp*-neutrino spectrum close to the end point contributes to the sensitive region in analysis) and $P^{2\nu}(862) = 0.55$ for ^{7}Be-neutrinos (higher energy line) is negligible. An estimate of $P^{2\nu} = 0.55$ was used in calculations.

The limits on the flavor magnetic moment can be obtained from (8) because individual contributions are positive. With $\mu_{\rm eff} < 2.8 \cdot 10^{-11}\mu_B$ and for $\sin^2\theta_{13} = 0.0210 \pm 0.0011$ and $\sin^2\theta_{23} = 0.51 \pm 0.04$ for normal hierarchy (or $\sin^2\theta_{23} = 0.50 \pm 0.04$ for inverted hierarchy) the following limits were obtained: $\mu_e < 3.9 \cdot 10^{-11}\mu_B$, $\mu_\mu < 5.8 \cdot 10^{-11}\mu_B$ and $\mu_\tau < 5.8 \cdot 10^{-11}\mu_B$, all at 90% C.L.

The values above were calculated for the choice of hierarchy providing a more conservative limit.

In another paper[28] the Borexino collaboration performed a search for the hidden antineutrino sources in the data. The presence of antineutrinos in original neutrino fluxes can be a consequence of neutrino electromagnetic interactions induced by the non-zero neutrino magnetic moment. The limit derived for solar antineutrino flux is 384 cm^{-2} s^{-1} (90% C.L.), assuming an undistorted solar ^{8}B neutrinos energy spectrum, corresponding to a neutrino-antineutrino transition probability $P_{\nu\to\overline{\nu}} < 7.2 \times 10^{-5}$ (90% C.L.) for E_ν above inverse beta-decay threshold of 1.8 MeV. Based on the upper limit of the antineutrino admixure in the Solar neutrino flux the following limit on the magnetic moment was obtained:

$$\mu_\nu < 6.0 \cdot 10^{-9} B_\perp[\text{kG}] \cdot \mu_B \ (90\%\ \text{CL}) \tag{9}$$

where $B_\perp$ is transverse component of the strength of the solar magnetic field. The estimates of B in the solar core varies by some orders of magnitude ranging from $B < 600$ G to $B < 7$ MG. These estimations correspond to upper limits of the neutrino magnetic moment between $1.0 \cdot 10^{-8}\mu_B$ and $8.5 \cdot 10^{-13}\mu_B$ (90% C.L.). The latter value is stronger than the current limit from astrophysical observations while the former limit is overlaid by other measurements.

4.4. *Neutrino non-standard interactions*

The observed neutrino contribution in Borexino spectra are determined by the fraction of the electron neutrino in the total neutrino flux at the surface of the Earth (or electron neutrino survival probability P_{ee}(E)), and the neutrino-electron scattering cross section defined by the chiral couplings of the neutrino and electron. Some theories beyond the Standard Model postulate the existence of Non-Standard Interactions (NSI's) which can modify the chiral couplings and P_{ee}. Phenomenologically, NSI's of the neutral current (NC) type are described by the Lagrangian density

$$\mathcal{L}_{\rm NSI} = -2\sqrt{2}G_F\varepsilon_{\alpha\beta}^{ff'C}(\bar{\nu}_\alpha\gamma^\mu\nu_\beta)(\bar{f}\gamma_\mu C f')$$

where $\alpha, \beta = e, \mu, \tau$ label the neutrino flavor, f and f' are leptons or quarks of the same charge but not necessarily the same flavor, C is the chirality of the ff' current (L or R), and $\varepsilon_{\alpha\beta}^{ff'C}$ is a dimensionless coupling constant parametrizing the strength of the NSI interaction normalized to G_F. In the Borexino data analysis

the attention was paid to the flavor-diagonal case $f = f' = e$ and $\alpha = \beta$, so it is convenient to denote $\varepsilon^{fC}_{\alpha\beta}$ as ε^{C}_{α}. Borexino, relying on neutrino-electron elastic scattering, is particularly sensitive to this type.

At detection, ε_α shifts the coupling constants that appear in the expression for the differential cross section for the weak interactions

$$g^C_\alpha \to \tilde{g}^C_\alpha = g^C_\alpha + \varepsilon^C_{\alpha\beta}$$

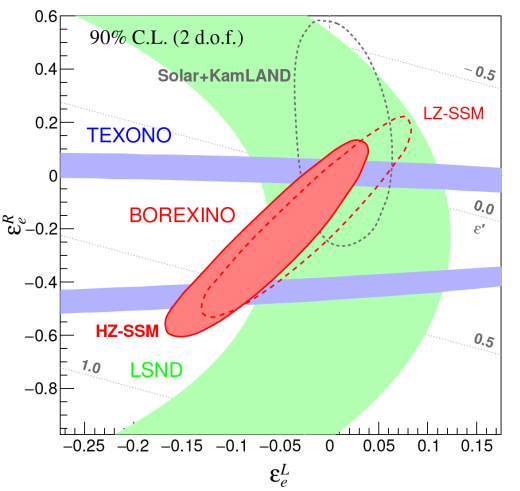

Fig. 5. Allowed region for NSI parameters in $\varepsilon^{L/R}_e$ plane obtained in.[29] The parameters $\varepsilon^{L/R}_\tau$ are fixed at zero. Both HZ- (filled red) and LZ- (dashed red) SSM's were considered. The bounds from the LSND and TEXONO experiments are provided for comparison. Besides, the contour obtained from the global analysis of solar neutrino experiments is presented by dashed black line,[30] NSI's are included in detection and propagation. All contours correspond to 90% C.L. (2 d.o.f.). The dotted gray lines represent the corresponding range of ε' parameter, relevant for NSI's at propagation.

The Borexino Phase II data data were used for the search of the flavor-diagonal neutral current interactions responsible for the ν_{ee} and and $\nu_{\tau e}$ couplings not excluded by other experiments. The solar luminosity constraints were implied to improve the sensitivity to the effects under study, both high- and low-metallicity (HZ and LZ) Standard Solar Model (SSM) predictions of the solar neutrino fluxes were considered. No indications of new physics were found at the level of sensitivity of the detector. The constraints on the parameters of the NSI's were obtained[29] compatible with or better than the existing ones. The results for $\varepsilon^{L/R}_e$ and $\varepsilon^{L/R}_\tau$ parameters are shown in Fig. 5 and Fig. 6 correspondingly.

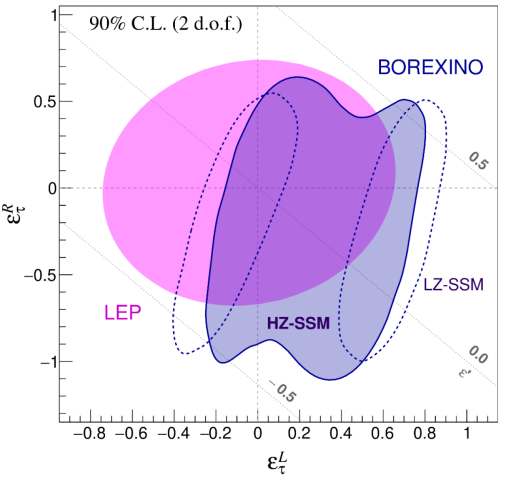

Fig. 6. Allowed region for NSI parameters in $\varepsilon_\tau^{L/R}$ plane obtained in.[29] The $\varepsilon_e^{L/R}$ are fixed at zero. Both HZ- (filled dark blue) and LZ- (dashed dark blue) SSM'sare considered. The contour from LEP experiment is provided for comparison. Both contours correspond to 90% C.L. (2 d.o.f.). The dotted gray lines represent the corresponding range of ε' parameter, relevant for NSI's at propagation.

5. High-energy solar neutrinos in Borexino

As already discussed, Borexino's original goal was the measurement of low energy solar neutrinos and this objective was fully centered. However, through the years, Borexino turned out to be a quite versatile experiment and the collaboration succeeded in measuring also neutrinos belonging to the above-MeV part of the solar neutrino spectrum. In particular, in 2020, Borexino presented a refinement of the measurement of the ^{8}B solar neutrino interaction rate,[31] also setting a new limit on the interaction rate of solar *hep* neutrinos.

The High-Energy Region (HER) work is based on 2062.4 live days of data, collected between January 2008 and December 2016 (detector's purifications and calibrations period excluded). In order to better handling the backgrounds, the analysis is performed with MonteCarlo radial fits, independently performed on two energy subranges: the HER-I (1650, 2950 p.e., roughly 3.2-5 MeV) and the HER-II (2950, 8500 p.e., roughly 5-16 MeV). The HER-I sector includes events originated from natural radioactivity while the HER-II sector is characterized by intense external γ rays following the neutron capture processes that happens on the Stainless Steel Sphere. In Borexino, the energy depositions of natural radioactivity never exceeds 5 MeV (Q-value of the ^{208}Tl β decay) since the α scintillation signals are strongly quenched and end below this analysis threshold. As of 2020, the ^{8}B neutrinos are detected via their elastic scattering off electrons on a fiducial mass of 300 t of liquid scintillator (the entire Borexino active mass) resulting in a total exposure of

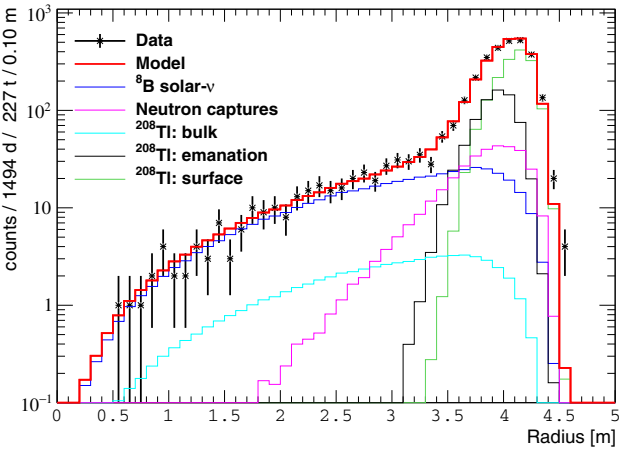

Fig. 7. Fit of the event radial distribution in the HER-I range[31] [1650,2950]p.e.

1.5 ktonne x year: an impressive 11.5-fold increase with respect to the previous Borexino ^{8}B measurement.[19]

In the HER analysis, the selection of data is performed via software cuts that tag/remove the primary/secondary backgrounds associated with the interaction of cosmic muons in the detector. The identification of the ^{8}B neutrino signal is then based on its different radial distribution with respect to that of background: neutrino events are expected to be uniformly distributed in the active volume while the remaining background event distribution is strongly radial dependent (Fig. 7).

The radial fit estimator is a binned likelihood and the χ^2/dof of the radial fits are 31.3/36 (HER-I), and 30.4/35 (HER-II) excluding empty bins.
The best-fit rates for the ^{8}B solar neutrinos are found to be:

$$R_{\mathrm{HER-I}} = 0.136\,^{+0.013}_{-0.013}\,(\mathrm{stat})\,^{+0.003}_{-0.003}\,(\mathrm{syst})\ \ \mathrm{cpd}/\,100\ \mathrm{t}$$
$$R_{\mathrm{HER-II}} = 0.087\,^{+0.080}_{-0.010}\,(\mathrm{stat})\,^{+0.005}_{-0.005}\,(\mathrm{syst})\ \ \mathrm{cpd}/\,100\ \mathrm{t}$$
$$R_{\mathrm{HER}} = 0.223\,^{+0.015}_{-0.016}\,(\mathrm{stat})\,^{+0.006}_{-0.006}\,(\mathrm{syst})\ \ \mathrm{cpd}/\,100\ \mathrm{t}$$

The precision of the HER ^{8}B rate analysis is then about 8% and it improves more than a factor 2 our previous result.[19] The equivalent ^{8}B neutrino flux inferred from the HER analysis[31] is $\Phi(^{8}\mathrm{B}) = 2.57\,^{+0.17}_{-0.18}\,(\mathrm{stat})\,^{+0.07}_{-0.07}\,(\mathrm{syst}) \times 10^{6}\ \mathrm{cm}^{-2}\,\mathrm{s}^{-1}$ well in agreement with the previous Borexino result[19] and with the high-precision measurement performed by Super Kamiokande.[32] The B16 HZ-SSM[7] expected ^{8}B neutrino flux is $5.46 \pm 0.66 \times 10^{6}\ \mathrm{cm}^{-2}\,\mathrm{s}^{-1}$ but the apparently missing flux is fully compatible the MSW-LMA neutrino oscillation scenario.

The Borexino experiment is not optimized for a clear detection of neutrino fluxes as low as those predicted by the SSM for the *hep* neutrinos ($\sim 10^{3}\ \mathrm{cm}^{-2}\,\mathrm{s}^{-1}$). Nevertheless, this elusive type of neutrinos is searched via their elastic scattering

on electrons as well as via their neutral current-mediated inelastic scattering on Carbon nuclei. The Borexino collaboration was able to set a limit on the number of expected *hep* events of 4.37 (90% C.L.), corresponding to a limit on the flux of $< 1.8 \times 10^5$ cm^{-2} s^{-1} which is about 1.2 times stronger than the one we previously reported in 2018.[11]

6. Conclusion and discussion

Solar neutrinos are an essential tool to understand stellar physics, being able at the same time to reveal some of their fundamental properties. The Borexino experiment, with its 14-years-long data taking, has been one of the key players in the investigation of these particles. Thanks to its outstanding radiopurity and to the deep understanding of the detector behaviour, Borexino has been able to overcome the intrinsic limitations of the previous generations of radiochemical experiments and to provide a precision measurement of all the components of the solar neutrino spectrum with the only exception of the very low flux of neutrinos from the Helium-proton fusion for which an upper limit has been set. In particular, in this contribution we report the Borexino results on neutrinos produced in the proton-proton fusion chain, which is by far the main energy production mechanism in our star. With a separate analysis of the low- and high-energy region of the energy spectrum, the individual fluxes of *pp*, *pep*, ^{7}Be and ^{8}B neutrinos were directly measured for the first time by a single experiment.

This result has significant implications for solar and particle physics: by measuring the flux of *pp* neutrinos with a 11% accuracy and the ^{7}Be flux with an unprecedented 3% precision, we could compute the luminosity of the Sun using neutrinos,[11] finding an excellent agreement with the photon-inferred result ($L_\odot^{\rm ph} = (3.846 \pm 0.015) \times 10^{33}\,{\rm erg\,s^{-1}}$ vs $L_\odot^{\nu} = (3.89^{+0.35}_{-0.42}) \times 10^{33}\,{\rm erg\,s^{-1}}$), thus confirming the nuclear origin of the solar power and the thermodynamical equilibrium of the Sun over the timescale required for radiation to flow from the core to the surface of the Sun, which is in the order of 10^5 years. Using the measurements of *pp* and ^{7}Be neutrino fluxes we could also study the relative weight of the two main terminations of the *pp*-chain (ppI and ppII in Fig. 1), which is the ratio $R_{\rm I/II}$ between the ^{3}He–^{4}He and ^{3}He–^{3}He fusion rates. Neglecting the small contribution of the ppIII branch and assuming the local kinetic equilibrium of ^{2}H and ^{3}He, we find $R_{\rm I/II} = 0.178^{+0.027}_{-0.023}$, in good agreement with the predictions of both the HZ and LZ SSM[11] ($R^{\rm HZ}_{\rm I/II} = 0.180 \pm 0.011$, $R^{\rm LZ}_{\rm I/II} = 0.161 \pm 0.010$). Furthermore, we could exploit the strong dependence of ^{7}Be and ^{8}B fluxes upon the Sun core temperature to test the predictions of the SSM implementing a different chemical composition. Changes in the Sun metallicity will indeed lead to different expectations of the temperature profile, affecting the expected neutrino fluxes. Borexino *pp*-chain results are compatible with the predictions of both HZ and LZ SSM,[11] but an hypothesis test show a mild preference for the higher core temperature expected from the HZ SSM.[11]

In its long scientific life, Borexino exceeded the expectations of its physics reach and is now among the leading solar neutrino experiments. This extraordinary journey recently culminated with the first observation of solar neutrinos from the CNO-cycle,[33] adding a new fundamental piece to our understanding of the Sun and of all stars.

Acknowledgements

The Borexino collaboration acknowledges the hospitality and support of the Laboratori Nazionali del Gran Sasso (Italy). The Borexino program is made possible by funding from Istituto Nazionale di Fisica Nucleare (INFN) (Italy), National Science Foundation (NSF) (USA), Deutsche Forschungsgemeinschaft (DFG) and Helmholtz-Gemeinschaft (HGF) (Germany), Russian Science Foundation (RSF) (grant number 21-12-00063), and Narodowe Centrum Nauki (NCN) (grant number UMO 2017/26/M/ST2/00915) (Poland).

References

1. A. Eddington, The Internal Constitution of the Stars, *Nature* **106** (1920).
2. A. Eddington, The internal constitution of the stars, *Observatory* **43** (1920).
3. H. Bethe and C. Critchfield, The Formation of Deuterons by Proton Combination, *Phys. Rev.* **54** (1938).
4. H. Bethe, Energy Production in Stars, *Phys. Rev.* **55** (1939).
5. C. von Weizsäcker, Über Elementumwandlungen in Innern der Sterne I, *Phys. Z.* (1937).
6. C. von Weizsäcker, Über Elementumwandlungen in Innern der Sterne II, *Phys. Z.* (1938).
7. N. Vinyoles, A. M. Serenelli, F. L. Villante, S. Basu, J. Bergström, M. C. Gonzalez-Garcia, M. Maltoni, C. Peña Garay and N. Song, A new Generation of Standard Solar Models, *Astrophys. J.* **835**, p. 202 (2017).
8. F. L. Villante, ecCNO Solar Neutrinos: A Challenge for Gigantic Ultra-Pure Liquid Scintillator Detectors, *Phys. Lett. B* **742**, 279 (2015).
9. M. Asplund, A. Grevesse, N.and Sauval and P. Scott, The chemical composition of the sun, *Annu. Rev. Astron. Astrophys.* **47** (2009).
10. N. Grevesse and A. Sauval, Standard solar composition, *Space Sci. Rev.* **85** (1998).
11. M. Agostini *et al.*, Comprehensive measurement of *pp*-chain solar neutrinos, *Nature* **562**, 505 (2018).
12. G. Alimonti *et al.*, The Borexino detector at the Laboratori Nazionali del Gran Sasso, *Nucl. Instrum. Meth. A* **600**, 568 (2009).
13. M. Agostini *et al.*, Modulations of the Cosmic Muon Signal in Ten Years of Borexino Data, *JCAP* **02**, p. 046 (2019).
14. M. Agostini *et al.*, First Simultaneous Precision Spectroscopy of *pp*, ^{7}Be, and *pep* Solar Neutrinos with Borexino Phase-II, *Phys. Rev. D* **100**, p. 082004 (2019).
15. M. Agostini *et al.*, The Monte Carlo simulation of the Borexino detector, *Astropart. Phys.* **97**, 136 (2018).
16. H. Back *et al.*, Borexino calibrations: Hardware, Methods, and Results, *JINST* **7**, p. P10018 (2012).

17. G. Bellini *et al.*, Final results of Borexino Phase-I on low-energy solar neutrino spectroscopy, *Phys. Rev. D* **89**, p. 112007 (Jun 2014).
18. C. Arpesella *et al.*, Direct Measurement of the Be-7 Solar Neutrino Flux with 192 Days of Borexino Data, *Phys. Rev. Lett.* **101**, p. 091302 (2008).
19. G. Bellini *et al.*, Measurement of the solar 8B neutrino rate with a liquid scintillator target and 3 MeV energy threshold in the Borexino detector, *Phys. Rev. D* **82**, p. 033006 (2010).
20. G. Bellini *et al.*, First evidence of *pep* solar neutrinos by direct detection in Borexino, *Phys. Rev. Lett.* **108**, p. 051302 (2012).
21. M. Agostini *et al.*, Identification of the cosmogenic ^{11}C background in large volumes of liquid scintillators with Borexino (6 2021).
22. I. Esteban, M. C. Gonzalez-Garcia, M. Maltoni, I. Martinez-Soler and T. Schwetz, Updated fit to three neutrino mixing: Exploring the accelerator-reactor complementarity, *JHEP* **01**, p. 087 (2017).
23. M. Agostini *et al.*, Seasonal modulation of the ^{7}Be solar neutrino rate in Borexino, *Astropart. Phys.* **92**, 21 (2017).
24. G. Bellini *et al.*, Absence of a day–night asymmetry in the ^{7}Be solar neutrino rate in Borexino, *Phys. Lett. B* **707**, 22 (2012).
25. E. Aprile *et al.*, Excess electronic recoil events in XENON1T, *Phys. Rev. D* **102**, p. 072004 (Oct 2020).
26. M. Agostini *et al.*, Limiting neutrino magnetic moments with Borexino Phase-II solar neutrino data, *Phys. Rev. D* **96**, p. 091103 (Nov 2017).
27. A. G. Beda *et al.*, Gemma experiment: The results of neutrino magnetic moment search, *Physics of Particles and Nuclei Letters* **10**, 139 (2013).
28. M. Agostini *et al.*, Search for low-energy neutrinos from astrophysical sources with borexino, *Astroparticle Physics* **125**, p. 102509 (2021).
29. M. Agostini *et al.*, Constraints on flavor-diagonal non-standard neutrino interactions from Borexino Phase-II, *J. High Energ. Phys.* **38** (2020).
30. A. Bolaños, O. G. Miranda, A. Palazzo, M. A. Tórtola and J. W. F. Valle, Probing nonstandard neutrino-electron interactions with solar and reactor neutrinos, *Phys. Rev. D* **79**, p. 113012 (Jun 2009).
31. M. Agostini *et al.*, Improved measurement of ^{8}B solar neutrinos with $1.5 kty$ of Borexino exposure, *Phys. Rev. D* **101**, p. 062001 (2020).
32. K. Abe *et al.*, Solar neutrino measurements in Super-Kamiokande-IV, *Phys. Rev. D* **94**, p. 052010 (Sep 2016).
33. M. Agostini *et al.*, Experimental evidence of neutrinos produced in the CNO fusion cycle in the Sun, *Nature* **587**, 577 (2020).